AIAA JOURNAL
Vol. 38, No. 11, November 2000

Nonlinear Finite Element Analysis of Machining and Sheet Metal Forming

V. Madhavan,* V. A. Gandikota,† and R. Agarwal‡
Wichita State University, Wichita, Kansas 67260-0035

Simulations are presented of machining and multistage sheet metal forming that improve on the accuracy of existing approaches by incorporating accurate representations of additional physical phenomena. In the finite element simulation of machining, chip formation is simulated without using a separation criterion. This capability has been successfully used to investigate fundamental aspects of machining such as the shape of the primary and secondary shear zones, chip curl, the size effect, and the uniqueness of machining. The analysis of multistage forming incorporates the effects of material property changes due to heat treatments between forming stages. Results of simulated forming operations are employed to evaluate the effectiveness of intermediate die shapes and heat treatments in improving the sheet metal formability. It is found that intermediate heat treatments enhance the ability of intermediate die shapes to promote uniform deformation of the sheet.

Introduction

MANY manufacturing processes involve complex interactions among a multitude of phenomena, such as plasticity, friction, heat generation, heat flow, material damage, phase changes, bifurcation, etc., that are dealt with in separate disciplines such as mechanics, tribology, heat transfer, materials science, and mathematics. Since the time of Tresca's[1] studies on the extrusion and machining of metals that led him to postulate the criterion for plastic deformation that carries his name, there have been significant improvements in our understanding of the manufacturing processes resulting from many advances in these disciplines. However, manufacturing processes, such as machining and sheet metal forming, for example, still pose ample challenges to researchers trying to analyze these processes accurately.

Currently the design and development of manufacturing processes in industry is primarily based on empirical knowledge, with additional experimentation carried out as needed. This approach is costly, time consuming, and leads to nonoptimal manufacturing. It is estimated[2] that the annual cost associated with machining and grinding in the United States alone is $115 billion. Thus, small increases in the efficiency of our manufacturing operations can result in significant savings.

Since the advent of modern computational analysis techniques, concerted efforts have been made to simulate and analyze manufacturing processes accurately. In this paper we describe the development of numerical techniques and computational codes for comprehensive analysis of machining without incorporation of a separation criterion and of multistage sheet metal forming including the effects of intermediate heat treatments. Continuous enhancements to the fidelity of analysis of manufacturing processes and determination of accurate values for critical inputs needed for these analyses are prerequisites for optimal design of manufacturing processes.

Background

Machining

The main approaches to modeling the physics of machining can be classified into the following analysis types.

Received 7 April 1999; revision received 23 February 2000; accepted for publication 26 February 2000.

*Assistant Professor, Department of Industrial and Manufacturing Engineering.

†Graduate Research Assistant, Department of Industrial and Manufacturing Engineering; currently Senior Engineer, Process, ESI Corporation, 570 Kirts Boulevard, Number 231, Troy, MI 48084.

‡Bloomfield Distinguished Professor and Executive Director, National Institute for Aviation Research. Fellow AIAA.

Slip-Line Field Analysis

The term slip-line field refers to two families of lines orthogonal to each other that represent the directions of maximum shear stress in a plastically deforming volume of material. The Hencky and Geiringer equations (see Ref. 3) can be used to obtain the cutting forces and hydrostatic stress and velocity fields and strain rates in the plastic zone. Various slip-line fields have been proposed for representing the deformation in machining. The radius of curvature of the cutting edge of the tool and the variation of the shear strength of the material with strain, strain rate, and temperature complicate the analysis tremendously.[4–6]

Mechanistic Models

In this commonly employed approach, machining is described as a combination of shear deformation at the primary deformation zone, shear and friction at the chip–tool interface, and indentation by the cutting edge.[7–10] These models usually have unknown constants that need to be obtained for each cutter geometry and material combination either by experimentation or from a database that can provide information about the shear angle, friction coefficient, and shear stress in orthogonal cutting. Such mechanistic models are descriptive in the sense that they cannot be used to predict the machining behavior of a new material based only on its properties.

Atomistic Analysis

Some researchers have modeled the machining process at the level of the individual atoms of the workpiece and the tool.[11–16] The tool and the workpiece are both modeled as separate collections of atoms. Each atom interacts with its neighbors according to assumed force laws that express the interatomic forces as functions of the interatomic spacing.

Cutting is simulated by forcing the atoms comprising the tool into the workpiece. It is observed that dislocations are generated at the cutting edge and move in a zigzag path to the free surface, resulting in a broad zone of shear as opposed to a shear plane. Upon continued infeed of the tool, a succession of progressive shearing motions are found to result in the formation of a chip. Note that no criterion for separation of the atoms is needed in these simulations.

Though this type of analysis can lead to accurate analysis on a small scale provided the interatomic force laws for the work material and for the chip–tool interface are accurately known, it is currently not possible to extend this analysis to the scales of most practical machining operations.

Finite Element Models

Various researchers[17–21] have carried out Lagrangian analyses of metal cutting incorporating the parting line concept. Usui and Shirakashi,[22] Obikawa and Usui,[23] and Maekawa et al.[24] have used material property values as a function of strain rate and temperature,

obtained from split Hopkinson bar tests. However, in their analyses also, a crack is introduced ahead of the cutting tool to allow material separation. It has been demonstrated that these analyses that incorporate node separation along a parting line neither reflect the true nature nor the magnitude of the stresses and strains found close to the cutting edge and, thus, do not simulate the machining process accurately.[25]

Eulerian analyses[26–28] can handle large deformations of the material because the mesh is fixed in space and the material flows through the mesh, thereby avoiding problems of mesh distortion and the need for a predefined parting line. However, such procedures require iterative modification of the assumed chip geometry to satisfy the velocity boundary conditions and typically cannot yield information about the residual stresses in the material. Marusich and Ortiz[29] have developed a Lagrangian finite element model of machining using continual remeshing and an explicit solution technique. Their model incorporates thermal effects as well as fracture criteria for the material and is able to predict localized shear deformation in the case of high-speed machining. Analysis of low-speed machining using these explicit solution techniques is computationally expensive.

From the considerations presented, it is clear that finite element analysis offers significant promise toward furthering our understanding of machining and for prediction of the outputs of the machining process. However, the accuracy of the analysis is principally dictated by how accurate a physical model of the machining process can be realized. Our model based on the many similarities observed between wedge indentation and cutting, obviates the need for artificially introducing a separation criterion for metal removal in machining. Elastic deformation, various plastic flow rules, arbitrary strain hardening, adhesion, friction, etc., and the dependence of these properties on temperature and strain rate can be modeled.

Sheet Metal Forming

Theoretical analysis of even simple metal forming operations necessitates broad assumptions to generate tractable governing equations.[30] Finite element analysis is the only practical tool for the analysis of realistic sheet metal forming operations with complex three-dimensional geometries, multiple forming steps, complex material models, etc., that has been proven by a number of studies.[31–33]

In the aerospace industry, many of the practical forming operations requiring the forming of aluminum sheets into complex geometries involve multiple forming stages with intermediate heat treatments between the stages, to avoid failure in the sheet. Though a vast amount of literature exists on various aspects of finite element analysis of sheet metal forming, very few researchers have addressed multistage forming simulations with intermediate annealing. This paucity may be attributable to the lack of use of intermediate annealing by the automotive industries, partially due to the higher formability of steels and partially due to the economics.

Logan et al.[34] and Thomas et al.[35] have used single-stage forming operations to estimate the number of forming stages, interstage anneals, and the punch depth for each preform. For this purpose they used a failure factor, defined as the ratio of the actual strain in the sheet to the failure strain given by forming limit diagrams. Wu and Yu[36] have analyzed the sequence of operations required for hydroforming a tubular engine cradle, but changes in the stress state due to unloading and material property changes due to intermediate heat treatments were not considered. It is known from a wide body of literature[31,37,38] that accurate representation of material properties is essential for accurate analysis of forming processes. It is, therefore, essential that finite element simulations of multistage forming operations should accurately represent the change in material properties due to any intermediate heat treatments.

Experimental information about changes in material properties due to intermediate heat treatments is limited. Gol'tsev et al.[39] and Takakura and Yamaguchi[40] used tensile tests to study the effects of intermediate solutionizing and annealing treatments on failure strains for aluminum alloys (D16AMO and JIS 13A). It was found in two-stage and three-stage tests that the total strain at failure increased with increasing values of strain in the initial stage(s), especially for solutionizing heat treatment.[39] This behavior could be modeled by defining an effectiveness coefficient to describe the ability of the heat treatment to reduce the effective plastic strains, thereby restoring ductility.

Parsa et al.[41] studied the effect of interstage annealing on the limiting redrawing ratio of cups using a two-dimensional rigid–plastic axisymmetric analysis. Annealing was represented by changes to values of the strength coefficient K and strain hardening exponent n and by zeroing out the plastic strain in the material model. This is equivalent to assuming an effectiveness coefficient of unity for the intermediate annealing process.

The experiments and simulations reviewed indicate the need for a capability to represent intermediate heat treatments accurately in full three-dimensional analyses of multistage sheet forming processes. We describe the development of such a capability for the widely used commercial software LS-DYNA. Simulations of multiple-stage forming of an aircraft engine nacelle inlet lip have been used to compare the effectiveness of intermediate die shapes to the effectiveness of intermediate material property changes in extending sheet metal formability.

Machining as a Wedge Indentation

Analysis Procedure

Based on similarities between experimentally observed deformation patterns in machining and indentation of ductile metals, and from atomistic analyses of these two processes, it has been shown that they are equivalent.[25] Therefore, finite element simulations of the machining of ductile materials that result in the production of continuous chips do not have to incorporate separation or failure criteria for the work material. As further proof, consider that many processes involving pure plastic deformation result in large amounts of new surface generation. For instance, if the length of an isotropic tension test specimen were doubled, the surface area increases by a factor of $\sqrt{2}$. In machining, the tool concentrates the new surface generation next to the cutting edge so that the new surfaces that are generated divide the material into the chip and the workpiece. Problems caused by mesh distortion due to intense localized deformation that occurs close to the cutting edge can be circumvented by remeshing and rezoning. On this basis, an iterative Lagrangian finite element model (FEM) has been developed that simulates machining using periodic remeshing of the workpiece to offset mesh distortions due to deformation caused by the infeed of the tool.

Cutting is simulated by forcing the tool to move into the workpiece in small increments. Contact elements prevent penetration of the tool into the workpiece and generate stresses that cause the work material to deform. When a predetermined value of the equivalent plastic strain is exceeded at any point in the workpiece, a new mesh is generated to represent the deformed configuration of the workpiece. During remeshing, the mesh is adaptively refined to make it finer in the regions of high gradients of stresses and strains, as well as in regions of high plastic strain increments, and coarse elsewhere. After interpolation of the stresses and strains onto the new mesh, the analysis is restarted by further infeed of the tool.

The method just described has been implemented using a combination of two commercial FEM packages. The creation and refinement of the meshes (preprocessing) and processing of the results (postprocessing) are both done using the P3/PATRAN package. The actual solution of each step in the simulation, when the tool is moved incrementally into the workpiece, is performed using ABAQUS. The use of commercial packages lends flexibility, robustness, and dependability to the analysis. For instance, recent changes permit the use of LS-DYNA as the solver so that explicit dynamic simulations can also be performed.

Blunt and sharp tools have been used to simulate the machining of perfectly plastic, as well as work hardening, materials. These simulations have reproduced many of the experimental observations and have been used to formulate novel explanations for some of these observations.

Results and Discussion

Figure 1 shows four different stages in the simulation describing the distribution of plastic strain, hydrostatic pressure, normal stress in the cutting direction x, and the von Mises stress, respectively. For this simulation, friction and adhesion at the chip–tool interface, work

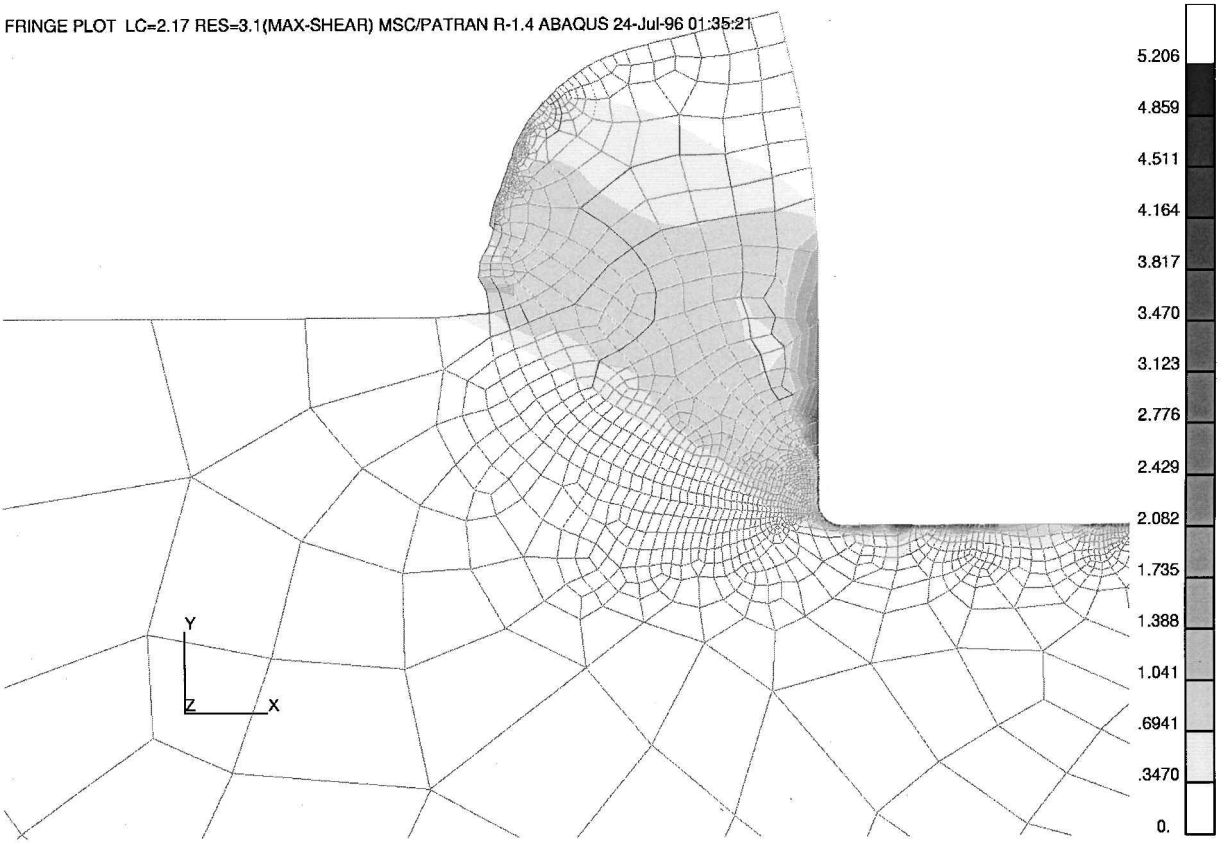

a) Distance cut = 0.35 mm, contours of plastic strain

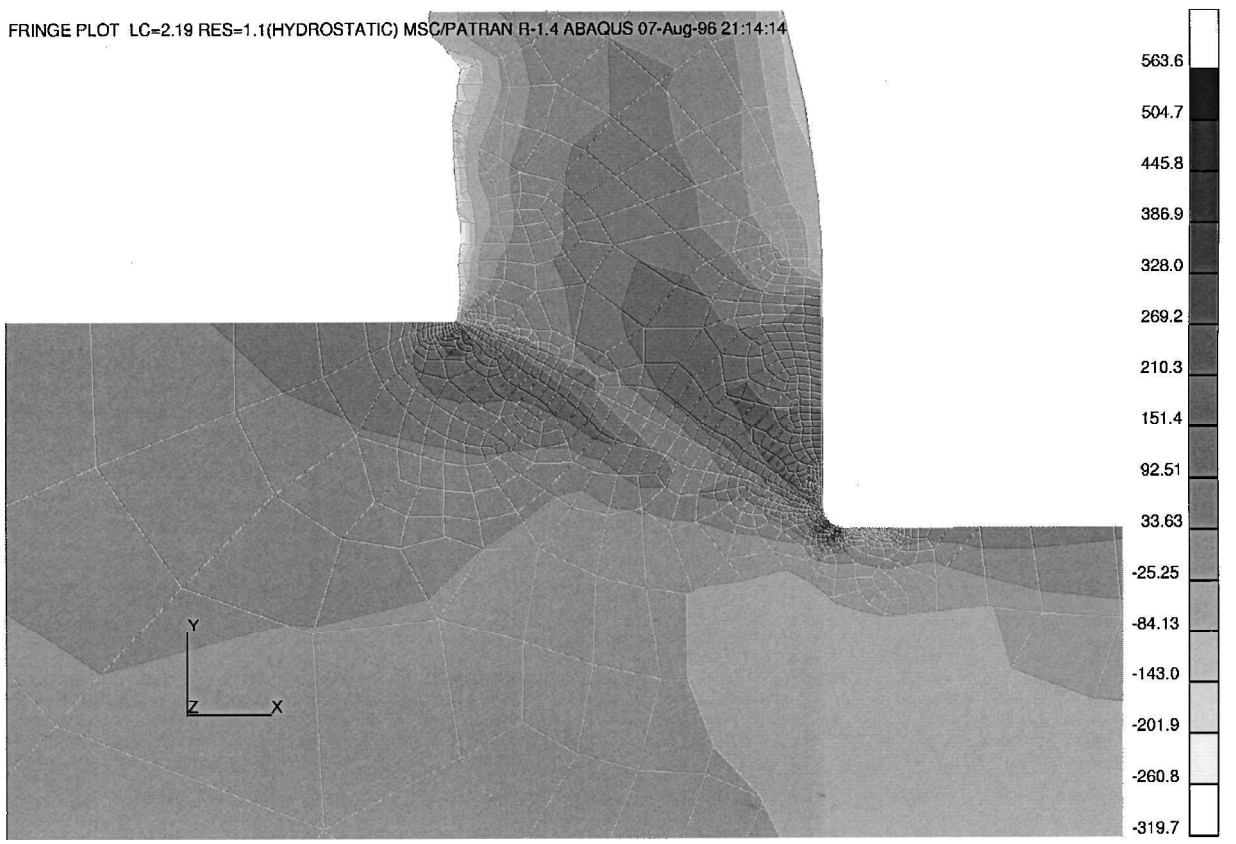

b) Distance cut = 0.88 mm, contours of hydrostatic pressure

Fig. 1 Stages in the simulation of machining with 20-θm tool cutting edge radius, 200-θm depth of cut, frictionless chip–tool contact, and elastic perfectly plastic work material with yield strength of 350 N/mm^2.

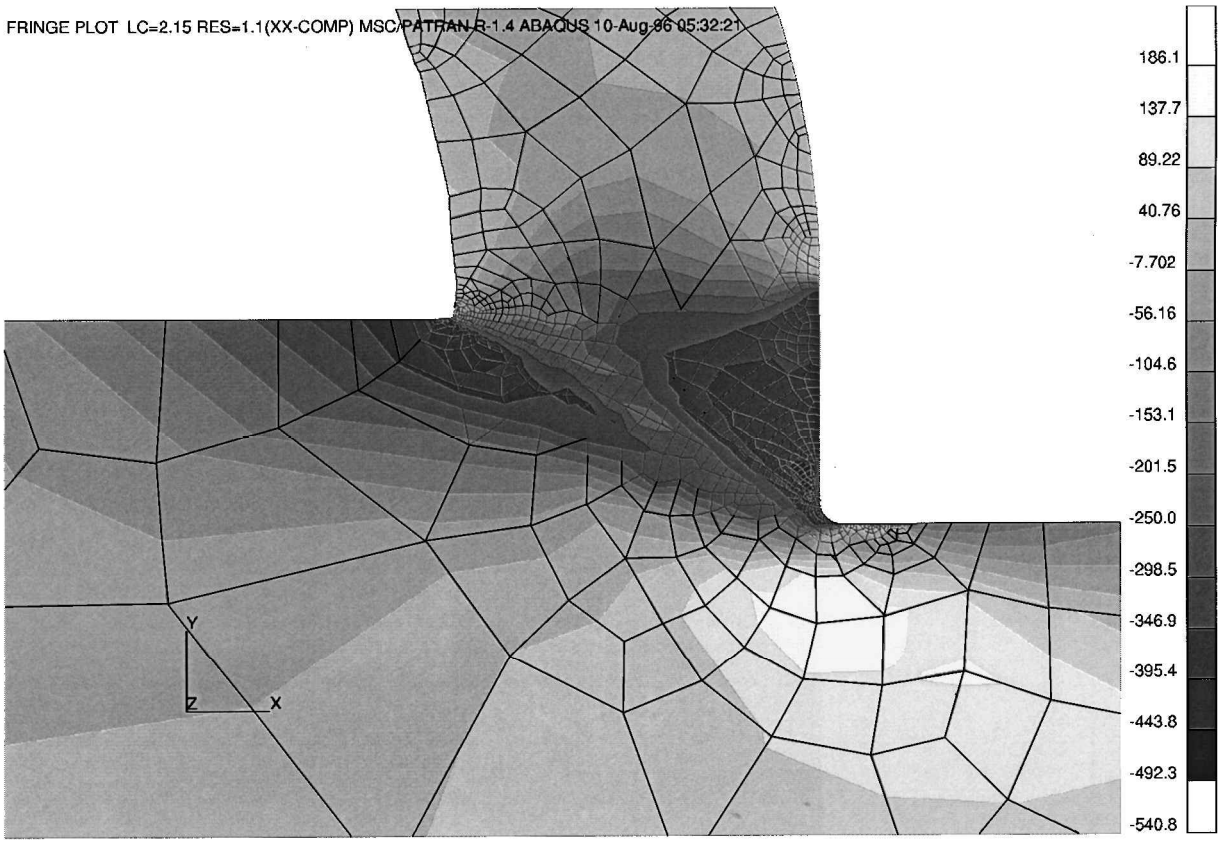

c) Distance cut = 1.21 mm, contours of σ_{xx}

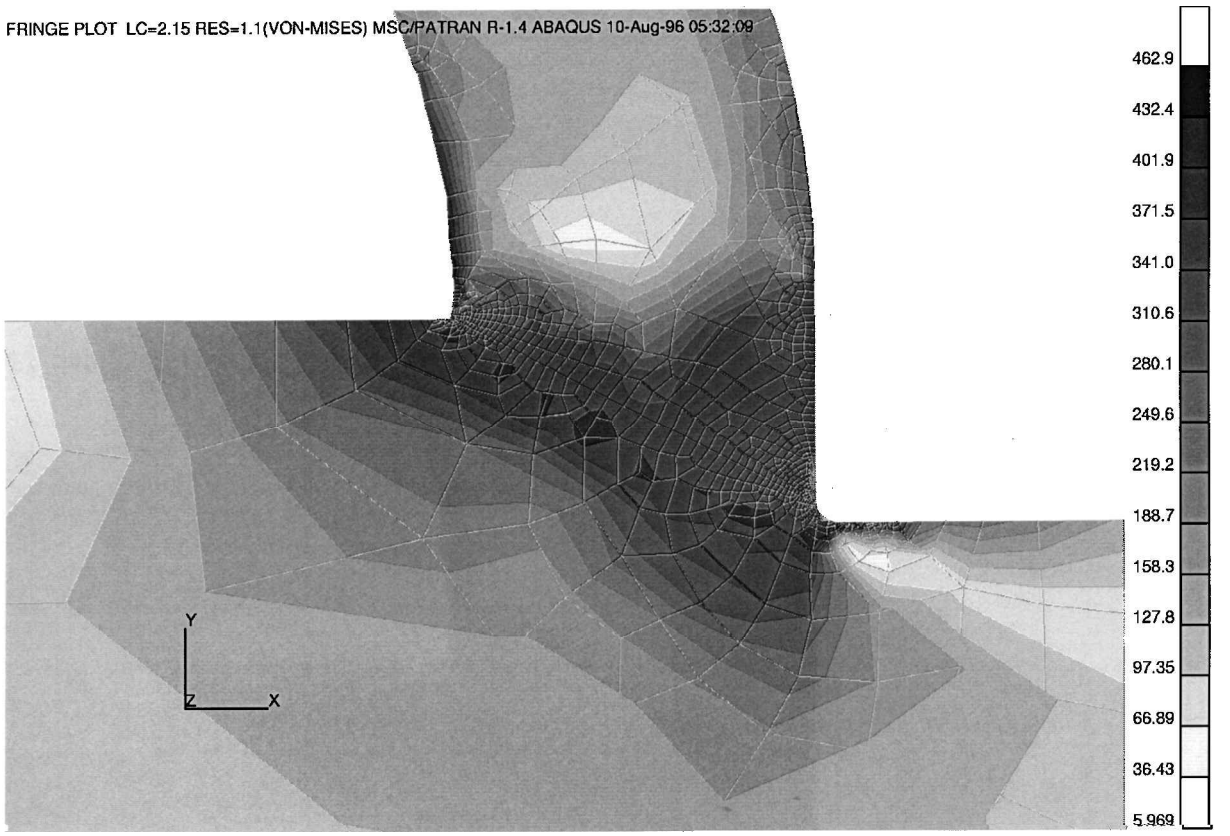

d) Distance cut = 1.74 mm, contours of effective stress

Fig. 1 Stages in the simulation of machining with 20-θm tool cutting edge radius, 200-θm depth of cut, frictionless chip–tool contact, and elastic perfectly plastic work material with yield strength of 350 N/mm^2 (continued).

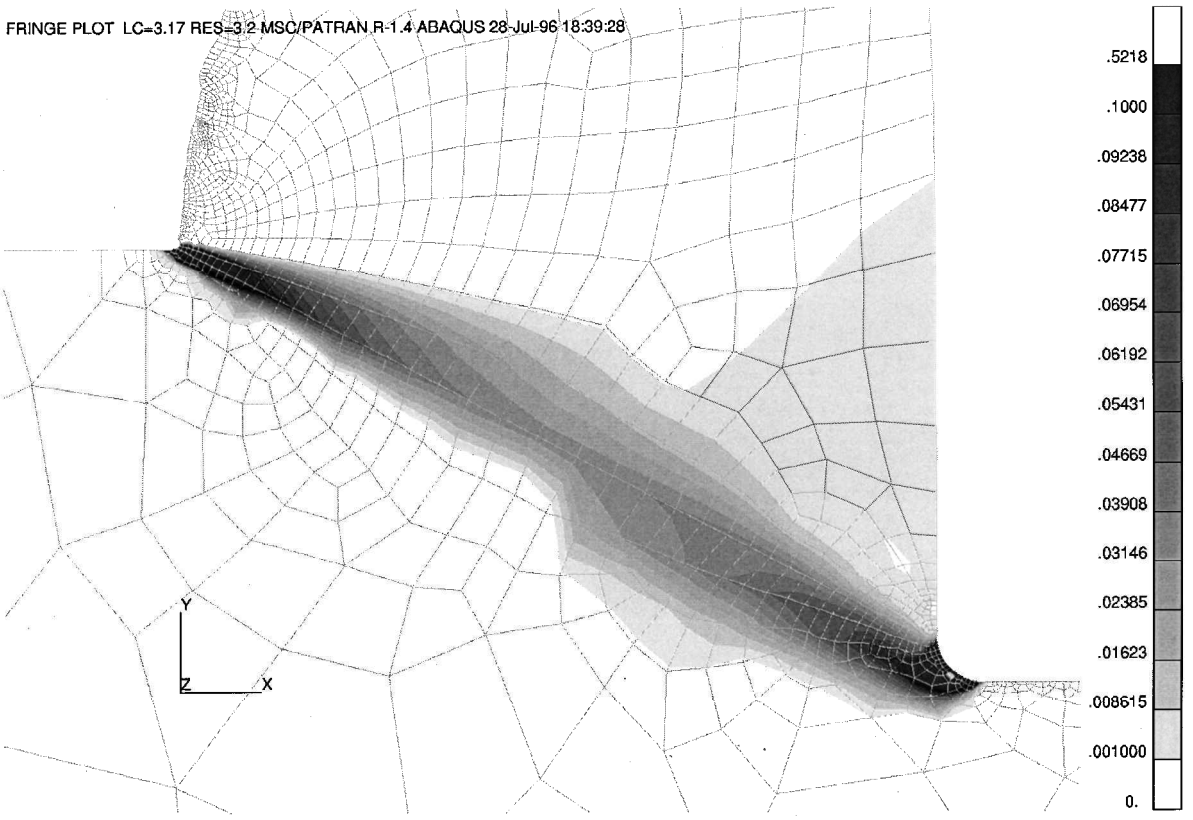

Fig. 2 Steady-state distribution of the increment of equivalent plastic strain within the workpiece during the 111th infeed of the tool: $\theta = 0$; distance cut = 0.63 mm.

material hardening, and temperature and strain rate effects were not considered. The yield strength of the material was assumed to be 350 N/mm^2. The cutting edge radius was taken to be 20 μm and the depth of cut was 200 μm.

The principal zones where deformation occurs are in a primary shear zone and in a triangular secondary shear zone near the rake face (Fig. 2) similar to those discussed elsewhere in the literature.[4,5,42,43] To note that the triangular secondary deformation zone exists even in the absence of friction between the chip and the tool, but produces very small magnitudes of strain so that it may not be detected by experimental techniques. The normal stress (Fig. 1c) on the tool rake face is uniformly high along the rake face except near the end of chip–tool contact where it rapidly decreases to zero. Friction at the chip–tool interface has been found to decrease chip curl and increase cutting forces.[25] The residual stress in the workpiece, when thermal effects are ignored in the analysis, is found to be compressive, as seen in Fig. 1c. The hydrostatic stress (Fig. 1b) is highly compressive near the cutting edge of the tool, decreases toward the middle of the primary shear zone, and then increases again near the shear plane exit (the place where the shear plane breaks out onto the free surface). Such a variation of the hydrostatic stress results in a shear zone (Fig. 2) that is similar in shape to the shear plane proposed by Dewhurst.[43] This curvature of the shear zone, mainly the decrease in the shear angle near the shear plane exit, seems to be the cause for chip curl.

A novel explanation for the size effect in machining has been formulated based on that deformation of work material close to the cutting edge of the tool is much higher than the average deformation in the chip, as seen in Fig. 1a. As the depth of cut and thus the thickness of the chip is reduced, the specific energy of machining will increase because a greater proportion of the material removed is highly strained. It has been observed in these simulations that as the cutting edge radius increases, the cutting force, the specific energy, and the average contact pressure increase, making the machining process more akin to indentation. The strain rate is also observed to vary across the chip cross section as can be inferred from the different widths of the primary shear zone (Fig. 2). The strain rate near the shear plane exit is very high and accompanying small-scale shear localization may be the reason that wrinkles are observed on the free surface of chips.

Because the finite element simulation described earlier has been shown to be capable of representing the physics behind machining with high fidelity, it is feasible to use this simulation to explore the uniqueness of the machining process. This has been carried out by perturbing the chip and observing the response of the process.[44]

Figure 3a shows the shape of the chip in the scenario in which it was artificially thickened and cutting resumed by further infeed of the tool. The thickness of the chip can be observed to have come back to its original unperturbed value. Figure 3b shows the complementary scenario wherein the abruptly thinned chip can be observed to have come back to its original thickness. From the sharpness of the transitions back to the normal thickness of the chip, it can be deduced that the normal mode of deformation is quite stable and that there are no other alternate stable modes of deformation. Experimental and theoretical studies[44] also indicate that the mode of deformation is indeed unique, and this uniqueness is possibly due to the applicability of the principle of minimization of energy to the machining process.

Simulation of Multistage Forming of an Engine Nacelle Inlet Lip

Analysis Procedure

In the production of many hydroformed components, the blank is deformed incrementally in several stages, with intermediate heat treatments, to reach the final shape of the component. The design of the die used in each of the stages determines the strain in that stage and the remaining ductility of the sheet. At the end of some of the stages of forming, the sheet is heat treated to increase its ductility, before the subsequent hydroforming stage.

We have developed a capability for analyzing multistage sheet forming accurately by incorporating the effects of material property changes due to various types of heat treatments between the forming stages. In each of the stages, the blank is formed to the shape of the

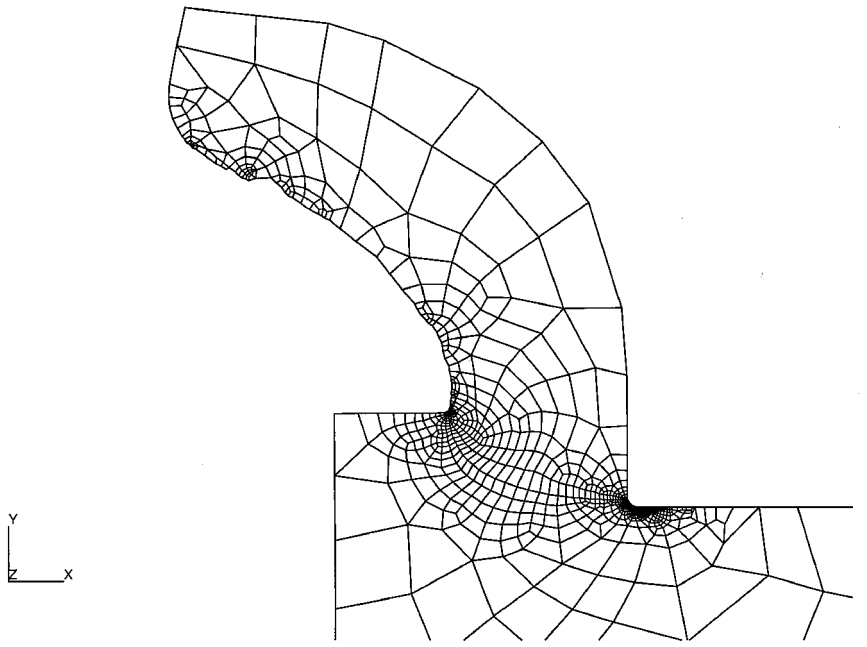

a) Steady-state shape of the chip after it was abruptly thickened

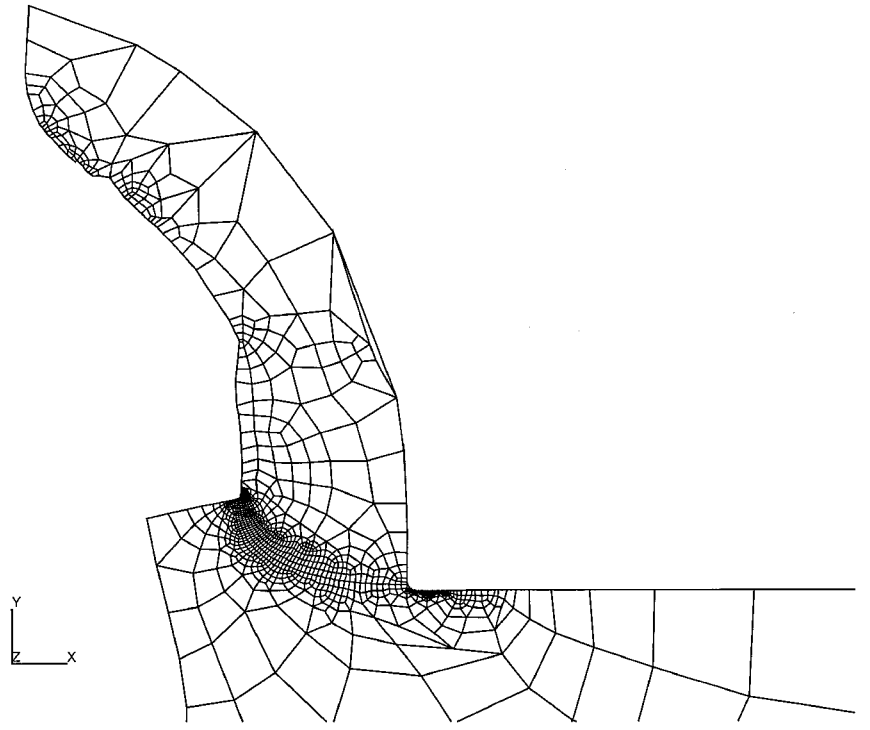

b) Steady-state shape of the chip after it was abruptly thinned

Fig. 3 Study of uniqueness of machining by perturbing the chip thickness.

die used in that stage by the application of pressure on one side (top) of the elements. At the end of the stage, the stresses in the elements are relieved and the strains are nullified while maintaining the deformed geometry of the part, including the sheet thickness variations. New material properties, corresponding to annealing or solutionizing treatment of the component, are used for the elements of the sheet, and changes to the die shape are incorporated. The simulation is then continued by applying pressure to the top of the elements representing the sheet.

In the present study, the commercial software package LS-DYNA is used to perform nonlinear explicit finite element analysis of sheet metal forming. Compared to implicit finite element analysis, explicit dynamic simulations have the inherent advantage of avoiding matrix inversions and iterations for nonlinear material properties and contact. The solution time for explicit dynamic simulations is proportional to the number of degrees of freedom, whereas it varies approximately as the third power of the number of degrees of freedom for implicit analyses.[32] Buckling and wrinkling can be simulated naturally using explicit dynamics. In addition a wide range of features are available within LS-DYNA, specifically tailored toward metal forming simulations. Hypermesh and PATRAN are the preprocessors used to model the geometry of the tools and the sheet and to generate the input files for LS-DYNA. The results are postprocessed using LS-TAURUS to produce stress, strain, force, pressure, and energy plots.

Simulation of multistage forming is accomplished by modifying an output file containing element stress and strain values that is written by LS-DYNA at the end of each stage of analysis and using it

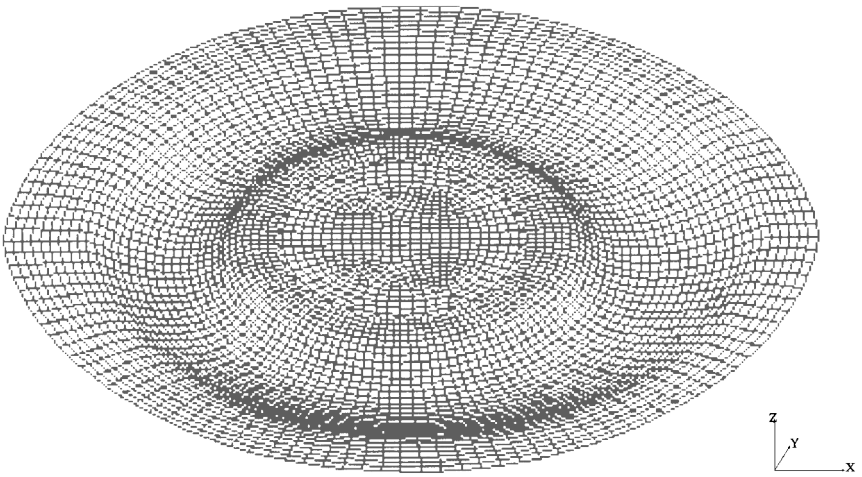

a) First stage

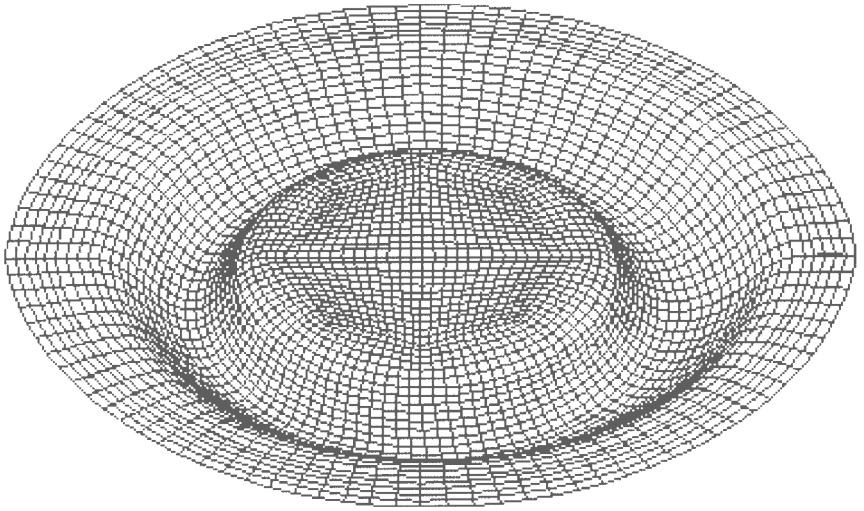

b) Second stage

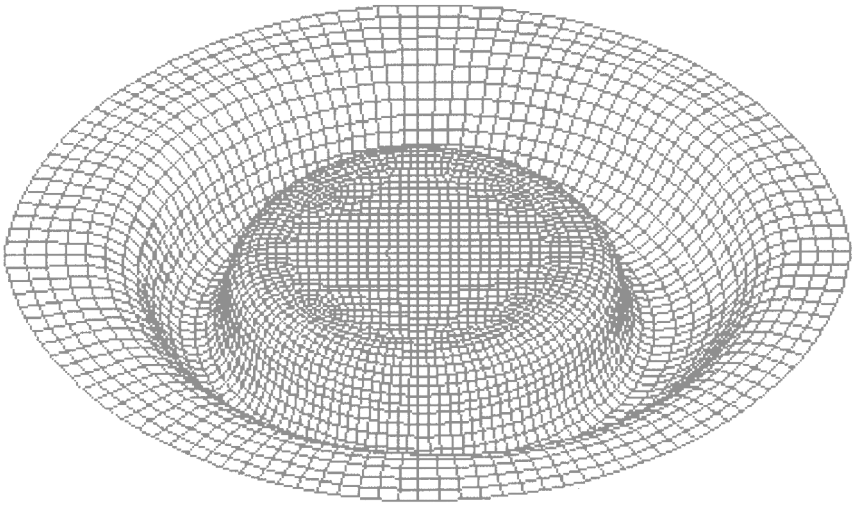

c) Third stage

Fig. 4 Shapes of the dies used for the three stages in the forming of the engine nacelle inlet lip.

as the input file for the next stage. Figure 4 shows the shapes of the first-, second-, and third-stage dies used for three-stage hydroforming of the engine nacelle inlet lip. The depths of these dies are 3.81, 8.13, and 11.68 cm, respectively. The blank is an elliptical annulus; the outer and inner major diameters are 104.1 and 21.3 cm, respectively. The thickness of the sheet is 1.6 mm. Because the die shapes are symmetric about the x–z plane, only one-half of the geometry is modeled. Symmetric boundary conditions are imposed on the sheet nodes along the line of symmetry, the x axis.

The FEM of the blank consists of 4420 four-noded Belytschko–Wong–Chiang elements with nine integration points through the thickness, whereas the dies are made up of 2252, 2002, and 2015 elements for the first, second, and third stages, respectively. The dies are specified to be rigid bodies, and all of the degrees of freedom are constrained.

The Barlat three-parameter material model is used to represent the anisotropic behavior of the 2024 aluminum alloy used for the sheet. The inputs to the material model obtained from uniaxial tension

Table 1 Material properties of 2024 aluminum in O and W conditions obtained from tension tests

Material type	E, GPa	ρ, kg/m^3	ν	K, MPa	n	R_{00}	R_{45}	R_{90}
Al 2024-O	64.9	2790	0.308	351	0.225	0.98	1.15	0.91
Al 2024-W	68.6	2790	0.312	779	0.337	0.78	1.12	0.86

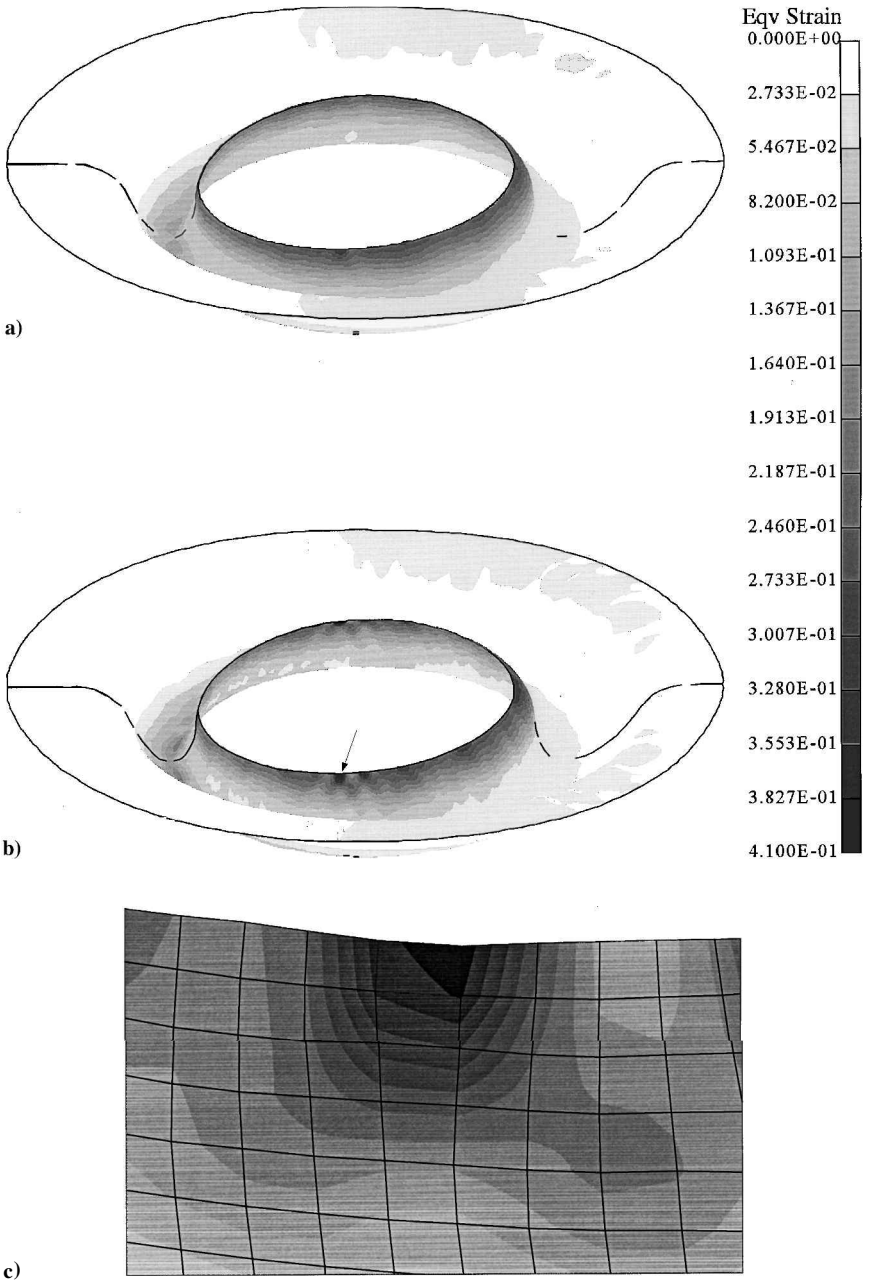

Fig. 5 Fringes of the increment in equivalent plastic strain during the third forming stage for the case when a) the sheet is annealed at the end of the first and second stages and b) the sheet is not annealed. The arrow in panel b points to the region of strain localization shown magnified in panel c.

tests along the 0-, 45-, and 90-deg directions in the plane of the sheet are given in Table 1. Coulomb friction at the contact between the sheet and die is modeled with static and dynamic friction coefficients equal to 0.05. The pressure on the sheet in each of the stages is ramped up from 0 to 13.79 MPa in 0.4 s, representing approximately a 10-fold speed up over the actual process. In addition, the density of the sheet material is scaled up 386 times, to speed up the explicit time stepping. Comparisons of the ratio of kinetic energy to internal energy of the sheet are used to ensure that inertial effects are negligible.

Results and Discussion

Effect of Intermediate Heat Treatments

Three different forming scenarios are simulated to compare the effect of annealing to the effect of intermediate die shapes on the strain distribution in the sheet. In the first scenario, the blank in the O-temper is formed to the shape of the first die, annealed back to the O-temper, formed to the shape of the second die, annealed, and formed to the final shape in the third stage. As already mentioned, annealing is accounted for by zeroing out the strains and the stresses in the sheet between the hydroforming stages.

Table 2 Results for maximum incremental and total equivalent plastic strains at the end of each of the three forming stages for the various scenarios considered

	Stage 1		Stage 2		Stage 3	
Forming type	Minimum	Maximum	Incremental maximum	Total maximum	Incremental maximum	Total maximum
Annealed	0.001	0.092	0.24	0.24	0.32	0.32
Unannealed	0.001	0.092	0.246	0.339	0.41	0.79
Single stage	0.008	2.203				

Table 3 Results for minimum and maximum sheet thickness at the end of each of the three forming stages for the various scenarios considered

	Stage 1		Stage 2		Stage 3	
Forming type	Minimum	Maximum	Minimum	Maximum	Minimum	Maximum
Annealed	1.42	1.52	1.25	1.58	1.07	1.62
Unannealed	1.42	1.52	1.23	1.58	0.95	1.61
Single stage	0.24	2.69				

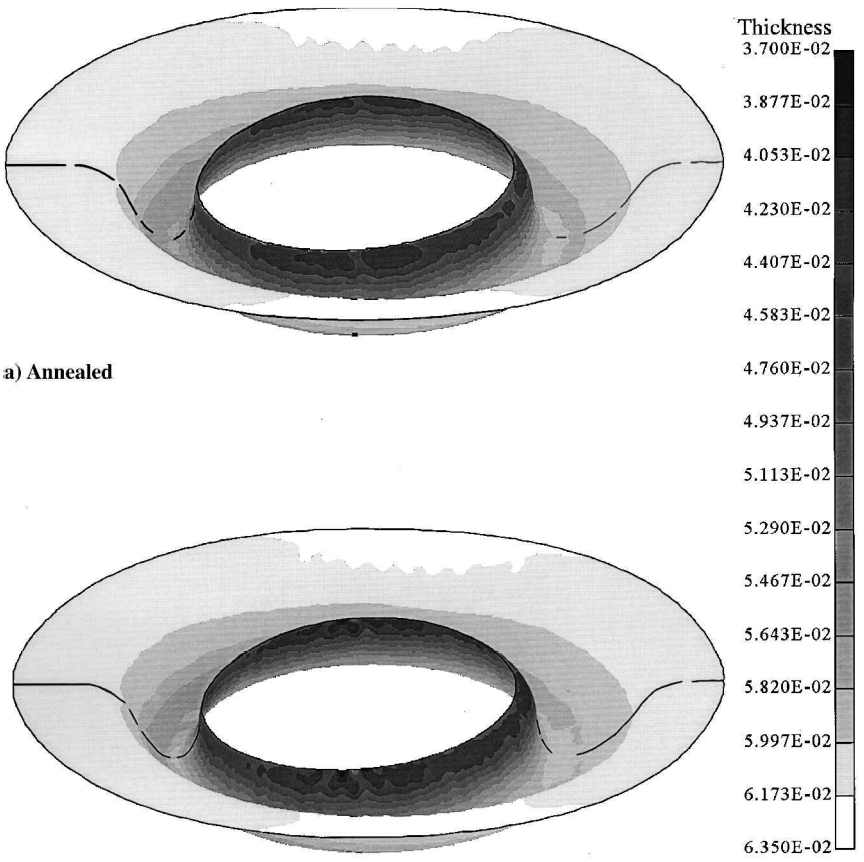

Fig. 6 Fringes of sheet thickness at the end of the third forming stage (in.).

In the second scenario, the intermediate heat treatments are neglected. The blank in the O-temper is formed sequentially to the shape of the first-, second-, and third-stage dies, without intermediate annealing. The equivalent plastic strain is not zeroed out and is allowed to accumulate through all of the stages.

Figures 5 and 6 show the effect of annealing between the hydroforming stages by presenting comparisons of the increment in equivalent plastic strain and sheet thickness, respectively, at the end of the analysis of the third forming stage. The fringe patterns shown in Figs. 5 and 6 provide a qualitative picture of the difference in deformation patterns caused by annealing.

Table 2 summarizes results for the maximum plastic strain and the maximum increment in plastic strain in each of the stages, and Table 3 summarizes results for sheet thickness at the end of each of the three stages, for the two scenarios with and without intermediate annealing. It can be observed from Table 3 that the minimum sheet thickness at the end of the second stage is similar for the analyses with and without annealing. A clearly discernible difference between the two scenarios is seen at the end of stage three due to the sharply lower sheet thickness in one particular region near the inner edge of the unannealed sheet, where localized necking has begun, as shown magnified in Fig. 4c. The maximum plastic strain increments for the two scenarios, with and without intermediate annealing, are significantly different at the end of both the second and third stages. It is always observed that the simulation of the scenario incorporating intermediate annealing shows a lower increment in plastic strain. This indicates that annealing leads to more uniform strain distributions within the sheet. A similar observation has also been

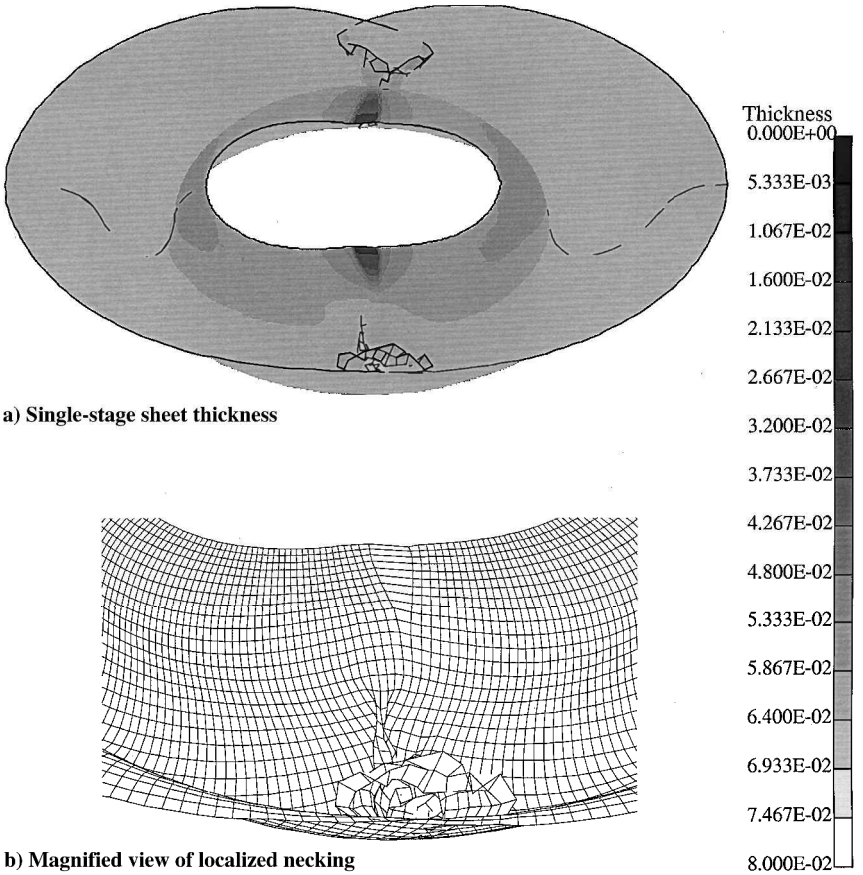

Fig. 7 Fringes of sheet thickness when the sheet is formed to the final geometry in a single stage; note wrinkles at the outer corner and localized necking in a region along the inner edge.

made by Parsa et al.,[41] albeit from the results of two-dimensional cup forming analysis. Note that the difference in strain increment between the annealed and unannealed forming operations is much higher for the third stage than for the second stage. This is again due to the localized necking already pointed out.

Effect of Intermediate Die Shapes

In the third scenario studied, the sheet is formed to the final shape in just one stage using the third-stage die of the three-stage analysis. The difference between this and the second scenario is that the sheet, while being formed to the final shape, is not forced to take on the shapes of the first and second dies. The deformed shape of the sheet and the results for sheet thickness at the end of single-stage forming to the final shape are presented in Fig. 7.

We can also observe from Tables 2 and 3 that the maximum plastic strain (2.203) in single-stage forming is much higher than the maximum accumulated strain (0.794) in the simulation without intermediate annealing. The minimum shell thickness is also observed to be much lower (0.24 mm compared to 0.95 mm), indicating highly localized deformation. Figure 7b is a magnified view of a region near the inner edge of the sheet produced in a single forming stage, where such localized necking of the sheet can be clearly observed. The results lead us to the conclusion that intermediate die shapes seem to promote a more uniform distribution of the strain in the sheet, by facilitating material flow from regions being compressed to those being stretched, while preventing wrinkling and the accompanying localized sheet thinning.

Conclusions

We have described an accurate FEM of machining wherein chip formation is simulated without recourse to separation criteria. This capability has been successfully used to investigate fundamental aspects of machining such as the shape of the primary and secondary shear zone, chip curl, the size effect, and the uniqueness of machining.

A capability for analyzing multistage forming accurately by incorporating the effects of property changes in between forming stages is also described. Application of this capability to analysis of multistage forming of an engine nacelle inlet lip shows that it is important to consider the effects of intermediate material property changes of the sheet in simulations to determine the number of stages needed for forming and the die shapes in those stages. The various scenarios simulated indicate that imposition of intermediate die shapes leads to more uniform deformation of the sheet. Intermediate heat treatments that nullify the plastic strains in the sheet enhance this effect.

The finite element simulation capabilities presented and the results of simulations discussed illustrate the need for accurate representation of a range of physical phenomena to ensure the fidelity of analyses of manufacturing processes. A predictive capability can be realized, provided standardized experimental techniques to determine the inputs for the finite element analyses are developed. For machining, such important inputs include the chip–tool contact conditions and temperature and strain-rate dependence of material properties. For sheet metal forming, friction, anisotropic material properties, and the effect of annealing on the pre-strained sheet are of importance. Once the accuracy of the inputs is ensured, experiments have to be conducted to study the accuracy of the simulation itself.

Transition from accurate analysis capability to an optimal design capability is yet to be tackled for the processes studied here. Present computational limitations do not allow utilization of such simulations in an optimization procedure, such as a gradient search technique, due to computational cost of these simulations. In the foreseeable future, it is anticipated that understanding of the physics of the processes, provided by a limited number of finite element analyses, will be used to establish design heuristics to guide the search for an optimum design of these manufacturing processes.

Acknowledgments

This work has been funded by grants provided by the Society of Manufacturing Engineers Educational Foundation, Kansas Science

and Technology Advanced Research (Kansas Experimental Program to Stimulate Competitive Research), and the Aircraft Design and Manufacturing Research Consortium, Wichita State University.

References

[1]Tresca, H., "Memoir on the Planing of Metals," Rept. of the U.S. Board Appointed to Test Iron, Steel, and Other Metals, Vol. 2, Government Printing Office, Washington, DC, 1881, pp. 617–685 (translated from French).

[2]Komanduri, R., "Machining and Grinding: A Historical Review of the Classical Papers," *Applied Mechanics Reviews*, Vol. 46, 1993, pp. 80–132.

[3]Kachanov, L. M., *Foundations of the Theory of Plasticity*, North-Holland, London, 1971, pp. 145–181.

[4]Palmer, W. B., and Oxley, P. L. B., "Mechanics of Metal Cutting," *Proceedings of the Institute of Mechanical Engineering*, Vol. 173, 1959, pp. 623–638.

[5]Roth, R. N., and Oxley, P. L. B., "A Slip-Line Field Analysis for Orthogonal Machining Based on Experimental Flow Fields," *Journal of Mechanical Engineering Science*, Vol. 14, 1972, pp. 85–97.

[6]Oxley, P. L. B., *The Mechanics of Machining: An Analytical Approach to Assessing Machinability*, E. Horwood, Chichester, England, U.K., 1989.

[7]Albrecht, P., "New Developments in the Theory of the Metal-Cutting Process. Part I—The Ploughing Process in Metal Cutting," *Journal of Engineering for Industry*, Vol. 82, 1960, pp. 348–358.

[8]Fu, H. J., DeVor, R. E., and Kapoor, S. G., "A Mechanistic Model for the Prediction of the Force System in Face Milling Operations," *Journal of Engineering for Industry*, Vol. 106, 1984, pp. 81–88.

[9]Budak, E., Altintas, Y., and Armarego, E. J. A., "Prediction of Milling Force Coefficients from Orthogonal Cutting Data," *Journal of Manufacturing Science and Engineering*, Vol. 118, 1996, pp. 216–224.

[10]Radulescu, R., and Kapoor, S. G., "An Analytical Model for Prediction of Tool Temperature Fields During Continuous and Interrupted Cutting," *Journal of Engineering for Industry*, Vol. 116, 1994, pp. 135–143.

[11]Belak, J. F., and Stowers, I. F., "A Molecular Dynamics Model of the Orthogonal Cutting Process," *Proceedings of the ASPE Fifth Annual Conference*, American Society for Precision Engineering, Raleigh, NC, 1990, pp. 259–264.

[12]Inamura, T., and Takezawa, N., "Atomic-Scale Cutting in a Computer Using Crystal Models of Copper and Diamond," *Annals of CIRP*, Vol. 41, No. 1, 1992, pp. 121–124.

[13]Ikawa, N., Shimada, S., Tanaka, H., and Ohmori, G., "An Atomistic Analysis of Nanometric Chip Removal as Affected by Tool-Work Interaction in Diamond Turning," *Annals of CIRP*, Vol. 40, No. 1, 1991, pp. 551–554.

[14]Inamura, T., Takezawa, N., and Kumaki, Y., "Mechanics and Energy Dissipation in Nanoscale Cutting," *Annals of CIRP*, Vol. 42, No. 1, 1993, pp. 79–82.

[15]Shimada, S., Ikawa, N., Tanaka, H., Ohmori, G., and Uchikoshi, J., "Feasibility Study on Ultimate Accuracy in Microcutting Using Molecular Dynamics Simulation," *Annals of CIRP*, Vol. 42, No. 1, 1993, pp. 91–94.

[16]Rentsch, R., and Inasaki, I., "Investigation of Surface Integrity by Molecular Dynamics Simulation," *Annals of CIRP*, Vol. 44, No. 1, 1995, pp. 295–298.

[17]Strenkowski, J. S., and Carroll, J. T., "A Finite Element Model of Orthogonal Metal Cutting," *Journal of Engineering for Industry*, Vol. 109, 1985, pp. 349–353.

[18]Shih, J. M., Chandrasekar, S., and Yang, T. Y., "Finite Element Simulation of Metal Cutting Process with Strain Rate and Temperature Effects," *Proceedings of the ASME Symposium on Fundamental Issues in Machining*, PED-Vol. 43, American Society of Mechanical Engineers, Fairfield, NJ, 1990, p. 11.

[19]Komvopoulos, K., and Erpenbeck, S. A., "Finite Element Modeling of Orthogonal Metal Cutting," *Journal of Engineering for Industry*, Vol. 113, 1991, pp. 253–267.

[20]Zhang, B., and Bagchi, A., "Finite Element Simulation of Chip Formation and Comparison with Machining Experiment," *Journal of Engineering for Industry*, Vol. 116, No. 3, 1994, pp. 289–297.

[21]Shih, A. J., "Finite Element Analysis of Orthogonal Metal Cutting Mechanics," *International Journal of Machine Tools and Manufacture*, Vol. 36, No. 2, 1996, pp. 255–273.

[22]Usui, E., and Shirakashi, T., "Mechanics of Machining—From 'Descriptive' to 'Predictive' Theory," *On the Art of Cutting Metals—75 Years Later*, PED-Vol. 7, American Society of Mechanical Engineers, Fairfield, NJ, 1982, pp. 13–35.

[23]Obikawa, T., and Usui, E., "Computational Machining of Titanium Alloy—Finite Element Modeling and a Few Results," *Journal of Engineering for Industry*, Vol. 118, 1996, pp. 208–215.

[24]Maekawa, K., Shirakashi, T., and Obikawa, T., "Recent Progress of Computer Aided Simulation of Chip Flow and Tool Damage in Metal Machining," *Proceedings of the Institution of Mechanical Engineers*, Vol. 210, 1996, pp. 233–242.

[25]Madhavan, V., Chandrasekar, S., and Farris, T. N., "Mechanistic Model of Machining as an Indentation Process," *Materials Issues in Machining—III and The Physics of Machining Processes—III*, edited by D. A. Stephenson and R. Stevenson, Metals, Minerals and Materials Society, Warrendale, PA, 1996, pp. 187–208.

[26]Carroll, J. T., and Strenkowski, J. S., "Finite Element Models of Orthogonal Cutting with Application to Single Point Diamond Turning," *International Journal of Mechanical Sciences*, Vol. 30, No. 2, 1988, pp. 899–920.

[27]Wu, J.-S., Dillon, O. W., and Lu, W.-Y., "Thermo-Viscoplastic Modeling of Machining Process Using a Mixed Finite Element Method," *Journal of Manufacturing Science and Engineering*, Vol. 118, 1996, pp. 470–482.

[28]Sekhon, G. S., and Chenot, J. L., "Numerical Simulation of Continuous Chip Formation During Non-Steady Orthogonal Cutting," *Engineering Computations*, Vol. 10, 1993, pp. 31–48.

[29]Marusich, T. D., and Ortiz, M., "Modelling and Simulation of High-Speed Machining," *International Journal for Numerical Methods in Engineering*, Vol. 38, 1995, pp. 3675–3694.

[30]Shang, H. M., Qin, S., and Tay, C. J., "Hydroforming Sheet Metal with Intermittent Changes in the Draw-In Condition of the Flange," *Journal of Materials Processing Technology*, Vol. 63, 1997, pp. 72–76.

[31]Slagter, W. J., and Thung, K. G., "Simulation of Sheet Metal Forming Processes Using MSC/DYTRAN," *Proceedings of Numisheet '96*, edited by J. K. Lee, G. L. Kinzel, and R. H. Wagoner, Ohio State Univ., Columbus, OH, 1996, pp. 394–402.

[32]Rebelo, N., Nagtegaal, J. C., Taylor, L. M., and Passmann, R., "Comparison of Implicit and Explicit Finite Element Methods in the Simulation of Metal Forming Processes," *Numerical Methods in Industrial Forming Processes*, edited by J.-L. Chenot, R. D. Wood, and O. C. Zienkiewicz, Balkema, Rotterdam, The Netherlands, 1996, pp. 99–108.

[33]Schrank, M. G., "Finite Element Modeling of the Hydroforming Press," TR KCP-613-4999, Allied Signal Aerospace Co., 1992.

[34]Logan, R. W., Thomas, D. B., and Young, G. K., "Implementation of a Pressure and Rate Dependent Forming Limit Diagram Model into NIKE and DYNA," *Concurrent Product and Process Engineering*, Vol. DE-Vol. 85, American Society of Mechanical Engineers, Fairfield, NJ, 1995, pp. 91–104.

[35]Thomas, D. B., Jr., Young, G. K., Larsen, R. C., and Firth, L., "Development and Optimization of an Aluminum Forming Process Using Finite Element Analysis as a Tool to Perform Parametric Studies," Society of Automotive Engineers, Paper 965554, 1996, pp. 1–6.

[36]Wu, L., and Yu, Y., "Computer Simulations of Forming Automotive Structural Parts by Hydroforming Process," *Proceedings of Numisheet '96*, edited by J. K. Lee, G. L. Kinzel, and R. H. Wagoner, Ohio State Univ., Columbus, OH, 1996, pp. 324–329.

[37]Hayashida, Y., Maeda, Y., Matsui, K., Hashimoto, N., Hattori, S., Yanagawa, M., Chung, K., Barlat, F., Brem, J. C., Lege, D. L., and Murtha, S. J., "FEM Analysis of Punch Stretching and Cup Drawing Tests for Aluminum Alloys Using a Planar Anisotropic Yield Function," *Simulation of Materials Processing: Theory, Methods and Applications*, edited by S. Shan-Fu and P. Dawson, Balkema, Rotterdam, The Netherlands, 1995, pp. 717–722.

[38]Barlat, F., Maeda, Y., Chung, K., Yanagawa, M., Brem, J. C., Hayashida, Y., Lege, D. J., Matsui, K., Murtha, S. J., Hattori, S., Becker, R. C., and Makosey, S., "Yield Function Development for Aluminum Alloy Sheets," *Journal of the Mechanics and Physics of Solids*, Vol. 45, No. 11/12, 1997, pp. 1727–1763.

[39]Gol'tsev, A. M., Del, G. D., and Eliseev, V. V., "Analysis of the Strain Capacity of Aluminum Alloy D16AMO," *Russian Metallurgy*, No. 3, 1989, pp. 75–78.

[40]Takakura, N., and Yamaguchi, K., "Effects of Interstage Annealing on Increase in Limit Strain of Alumimum Sheets," *Journal of Japan Institute of Light Metals*, Vol. 44, No. 1, 1994, pp. 41–47 (in Japanese).

[41]Parsa, M. H., Yamaguchi, K., Takakura, N., and Imatani, S., "Consideration of the Re-Drawing of Sheet Metals Based on Finite-Element Simulation," *Journal of Materials Processing Technology*, Vol. 47, No. 1, 1994, pp. 87–101.

[42]Kudo, H., "Some New Slip-Line Solutions for Two-Dimensional Steady-State Machining," *International Journal of Mechanical Sciences*, Vol. 7, 1965, pp. 43–55.

[43]Dewhurst, P., "On the Non-Uniqueness of the Machining Process," *Proceedings of the Royal Society of London, Series A: Mathematical and Physical Sciences*, Vol. 360, 1978, p. 587.

[44]Madhavan, V., and Chandrasekar, S., "Some Observations on the Uniqueness of Machining," *Predictable Modeling of Metal Cutting as a Means of Bridging the Gap Between Theory and Practice*, edited by V. Astakhov, MED-Vol. 6-2, American Society of Mechanical Engineers, Fairfield, NJ, 1997, pp. 99–109.

A. N. Palazotto
Associate Editor